Coordinated Broadcasting for Multiuser Indoor Visible Light Communication Systems

Hao Ma, *Student Member, IEEE*, Lutz Lampe, *Senior Member, IEEE*, and Steve Hranilovic, *Senior Member, IEEE*

***Abstract*—Visible light communication (VLC) re-uses illumination devices, in particular light-emitting diodes (LEDs), for communication purposes. It has great potential to alleviate the strain on radio frequency spectrum in indoor environments. VLC-enabled LED luminaries form VLC attocells that carry downlink data traffic to indoor mobile or stationary terminals. While one of the advantages of indoor VLC is low interference due to natural cell boundaries such as walls, multiple VLC attocells within a room would interfere. This is because illumination requirements often mandate a rich overlap of emissions of luminaries in a room. In this paper, we suggest the coordination of multiple VLC attocells (i.e., VLC-enabled LED luminaries) to turn the problem of overlap and thus interference into an advantage. We stipulate that this coordination can be accomplished through power line communication (PLC), which has been considered before as a means to transport data to VLC transmitters. Borrowing from concepts developed for radio-frequency wireless communications, we develop several precoding schemes for the new coordinated VLC broadcasting architecture. These include designs for the case of imperfect channel knowledge at the VLC transmitter, since channel information is usually provided through a low-rate feedback channel. The performance advantages for VLC transmission due to the proposed coordination and precoding designs are demonstrated based on a set of numerical results.**

***Index Terms*—Visible light communication (VLC), multiuser communications, precoding, broadcasting, imperfect channel state information.**

I. Introduction

Wireless data traffic is increasing at a fast pace, with most of the traffic being generated in homes, office buildings and other indoor spaces [2]. The creation of small-cell networks and operation of heterogeneous networks are two means to address this problem. However, eventually the usable radio-frequency (RF) spectrum is a finite resource and inter- and intra-cell interference are limiting wireless network capacity.

A mostly untapped resource that could alleviate the strain on RF spectrum is optical wireless communication (OWC), and in particular visible light communication (VLC) for indoor wireless transmission. VLC operates over the license-free visible spectrum and thus does not cause interference to RF wireless signals. Also interference between VLC transmitters is confined to within rooms or otherwise walled areas. VLC uses light-emitting diodes (LEDs) as the transmitting devices. The information-carrying signal modulates the light carrier by varying illumination intensity, i.e., the brightness of the LED signal, fast enough to be imperceptible by humans. Since LEDs are replacing incandescent bulbs and fluorescent lamps for illumination, VLC emitters will be ubiquitously available. At the receiver side, an inexpensive photodetector converts the optical signals into electrical signals to decode the information. Thus, virtually any device can be enabled to become a VLC receiver at minimal cost. Furthermore, both industrial activity and standardization around VLC is rapidly maturing, cf. e.g. [3], [4].

The integration of VLC into an indoor communication network establishes optical attocells [5], responsible for the downlink traffic from network to user terminals. These attocells could be easily deployed wherever LEDs are adopted for general illumination, including in electromagnetic interference sensitive areas like hospitals and airplanes. Although opaque boundaries effectively contain light signals, VLC attocells would generally not operate free of interference. Illumination designers aim to have a uniform illumination at a certain height in a room. This mandates a rich overlap between the emissions of luminaries to make illumination more uniform. Therefore, interference between VLC emitters is unavoidable. Fortunately, this interference will be spatially limited to neighboring or nearby attocells.

In this paper, we consider VLC attocell systems and propose the coordination of different transmitters, i.e., LED luminaries, through a backbone network. The purpose of this coordination is to turn unwanted interference into constructive signal components. The backbone could be realized by a wired Ethernet or power-over-Ethernet link. Another convenient manner to realize the backbone is using existing electrical power wiring for data communications, i.e., power line communications (PLC) [6]. The concept of integrating PLC and VLC to form a hybrid system for fast data delivery to users in indoor office buildings and homes is not new [7]–[9]. However, we suggest that since multiple LED luminaries in the same room are connected to the same power wires, PLC can be used to serve as a backbone network to support the cooperation among multiple VLC attocells. This was first mentioned in our conference paper [10], and can be considered as the VLC counterpart to *coordinated multipoint* (CoMP) in RF cellular networks [11].

Multiple coordinated VLC emitters form a virtual multiple-transmitter (or multiple-"antenna") system. In this paper, we focus on the signal processing required at the VLC transmitters

Manuscript received August 24, 2014; revised January 9 and May 8, 2015. This work was supported by the Natural Sciences and Engineering Research Council (NSERC) of Canada.

H. Ma and L. Lampe are with the Department of Electrical and Computer Engineering, University of British Columbia, Canada. S. Hranilovic is with the Department of Electrical and Computer Engineering, McMaster University, Canada. Email: haoma@ece.ubc.ca, Lampe@ece.ubc.ca, hranilovic@mcmaster.ca

Parts of this work have been presented at the IEEE Global Communications Conference (Globecom), Workshop on Optical Wireless Communications (GC13 WS - OWC), Atlanta, GA, USA, December 2013 [1].

to benefit from coordination [1]. We note that this is quite different from the indoor multiple-input multiple-output (MIMO) VLC systems for point-to-point communication studied in [12], [13], as we are dealing with broadcasting of data to multiple VLC receivers (e.g. cellular phones or tablets) employing single photodiode receivers. Such multiuser multiple-input single-output (MU-MISO) systems have widely been studied for radio communication systems, cf. e.g. [14]–[16]. However, different from RF wireless communication, VLC uses intensity modulation and the transmitted signal must be non-negative and constrained in mean amplitude, i.e., average optical power. These differences render solutions developed for the RF case not directly applicable to VLC systems. We investigate the effect of different levels of coordination of luminaries in a room, leading to different numbers of attocells and intercell-interference scenarios. Within a coordinated broadcasting system, linear minimum mean-squared error (MMSE) precoder design is applied. This allows us to consider interference from adjacent VLC transmitters that are not coordinated, as well as ambient light from the sun and other non-VLC lighting devices. Furthermore, we extend our design to the case of imperfect knowledge of the VLC transmission channel. Our numerical results highlight the benefits of coordination for VLC attocell systems by demonstrating significant gains in achievable signal-to-interference-plus-noise ratio (SINR). Finally, we note that our work is related and extends beyond the study in [17], which appeared parallel to our work [1] and considered MU-MISO transmission for VLC with zero-forcing precoding.

The remainder of the paper is organized as follows. In Section II, we propose a coordinated VLC system architecture with PLC as its backbone network. In Section III, precoder design strategies for VLC MU-MISO transmission with perfect channel state information (CSI) at the transmitter are developed. In Section IV, the designs are extended to the case of imperfect CSI. Simulation results are presented and discussed in Section V, and finally we conclude this paper in Section VI.

The following notations are used in this paper. Bold uppercase and lower case letters are used to denote matrices and vectors, respectively. vec$(\cdot)$ is the vectorization operator, $\otimes$ represents the Kronecker product, and $\boldsymbol{I}$ and $\mathbf{1}$ are the identity matrix and all-one vector of appropriate size, respectively. $\|\cdot\|_p$ represents the p-norm, $[\cdot]^T$ is the transpose operator, and $\mathbb{E}(\cdot)$ denotes statistical expectation.

II. Coordinated VLC Broadcasting

We consider an indoor environment with multiple LED luminaries deployed in a room, office, laboratory or similar indoor space. The main elements of the coordinated VLC broadcast system are illustrated in Figure 1. The luminaries function as VLC transmitters as a secondary use, and they receive electricity and data through a PLC backbone network. This enables some of the VLC transmitters, e.g., those connected to the same distribution box, to operate in a coordinated fashion alike CoMP. Similar to the definition of a CoMP-cell in the context of RF wireless systems [11], we define a

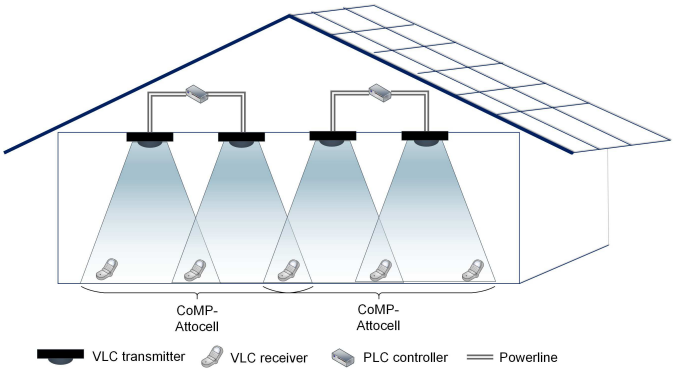

Figure 1: Illustration of indoor coordinated VLC broadcast system.

CoMP-attocell as the area covered by one VLC broadcasting system where all the transmitters are coordinated by the PLC backbone network. In the case of multiple CoMP-attocells in one room, there is interference from neighbouring CoMP-attocells, which is analogous to inter-CoMP-cell interference in RF cellular systems.

A. VLC Channel

Before discussing the broadcast transmission and VLC-specific constraints, we first briefly elaborate on channel gain and noise models applicable to intensity modulation (IM) at the transmitter and direct detection (DD) at the receiver (IM/DD).

Each LED luminary has K LED elements with a Lambertian radiation pattern. We consider the use of commercial off-the-shelf LEDs, whose bandwidth can reach up to 20 MHz [18]. In this case, multipath delay resulting from wall reflections and the path difference among spatially separated LED luminaries can be ignored and the VLC channel can be approximated as a single-tap channel. The channel gain h_{kn} between the k_{th} receiver and the n_{th} LED luminary can be expressed as [19]

$$h_{kn} = \sum_{i=1}^{K} \frac{G_{kn} A_k}{D_{kn_i}^2} R(\phi_{kn_i}) T(\psi_{kn_i}) \cos(\psi_{kn_i}) \mathbb{I}_{\mathcal{A}}(\psi_{kn_i}) \,, \tag{1}$$

where $G_{kn} = \gamma_k s_n$ comprises the photodetector responsivity γ_k [A/W] and LED conversion factor s_n [W/A], D_{kn_i} is the distance between the k_{th} receiver and the i_{th} LED in the n_{th} LED luminary, ψ_{kn_i} is the angle of incidence at which the light is received relative to the normal vector of the receiver plane, ϕ_{kn_i} is the angle of irradiance at which the light is emitted relative to the normal vector of the transmitter plane. $T(\psi_{kn_i})$ is the gain of the optical filter at the receiver. Furthermore, $\mathbb{I}_{\mathcal{A}}(\psi_{kn_i})$ denotes the indicator function, and $\mathcal{A} = \{\psi_{kn_i} | \, 0 \leq \psi_{kn_i} \leq \psi_c\}$, where ψ_c is the width of the field of view (FOV) at a receiver. The Lambertian radiant intensity is given by

$$R(\phi_{kn_i}) = \frac{(m+1)\cos^m(\phi_{kn_i})}{2\pi}, \tag{2}$$

where m is the Lambertian order and specifies the transmit

beam divergence:

$$m = -\frac{\log(2)}{\log(\cos(\phi_{\frac{1}{2}}))} , \tag{3}$$

where $\phi_{\frac{1}{2}}$ is the transmitter semiangle. The receiver collection area A_k of the k_{th} user can be expressed as

$$A_k = \frac{\kappa^2}{\sin^2(\psi_c)} A_{\text{PD}}^k, \tag{4}$$

where A_{PD}^k is the area of photodetector and κ is the concentrator refractive index.

The receiver-side noise term z_k (see (12) below) can be written as

$$z_k = i_k + n_k , \tag{5}$$

where i_k is the interference from neighbouring CoMP-attocells with average received electrical power $\mathbb{E}(i_k^2) = \sigma_{i_k}^2$, and the VLC noise component n_k comprises shot and thermal noise. We assume that n_k can be modelled as zero-mean Gaussian variable with variance [20]

$$\sigma_{n_k}^2 = 2eB(I_{\text{rp}}^k + I_{\text{bg}} I_2) + \sigma_{\text{th}}^2 , \tag{6}$$

where e is the elementary charge, B is system bandwidth, I_{bg} is background current, I_2 is the noise bandwidth factor (second Personick integral [21]), and σ_{th}^2 is the thermal-noise variance. I_{rp}^k is the average current due to the useful received signal at the k_{th} receiver. Denoting N_{t} the number of LED luminaries in one CoMP-attocell and I_{DC}^n the DC current of the n_{th} LED luminary, I_{rp}^k is given by

$$I_{\text{rp}}^k = \sum_{n=1}^{N_{\text{t}}} I_{\text{DC}}^n h_{kn} . \tag{7}$$

We observe that I_{rp}^k is dependent on the DC current and thus illumination level and on user location, via h_{kn}. This renders the optimization of broadcast transmission intractable. Therefore, we will use a fixed upper bound for I_{rp}^k in the following optimization. The accurate noise power is however applied for all numerical results.

Finally, we denote the total interference and noise power as

$$\sigma_k^2 = \mathbb{E}(z_k^2) = \sigma_{i_k}^2 + \sigma_{n_k}^2 . \tag{8}$$

B. Broadcast Transmission

In a VLC CoMP-attocell, N_{t} LED luminaries cooperate to broadcast information to N_{r} single-photodiode users. On-off keying (OOK) is applied in this work due to its popularity in optical communications and ease of implementation [22].[1] This is accomplished by modulating a zero-mean data signal onto the DC bias currents $\boldsymbol{I}_{\text{DC}} = [I_{\text{DC}}^1, \ldots, I_{\text{DC}}^{N_{\text{t}}}]^T$, which determine the brightness levels of the N_{t} LED luminaries. In the following, we describe the pre-processing of this data signal.

Let us denote $d_k \in \{\pm 1\}$ the binary data symbol intended for the k_{th} user, and $\boldsymbol{d} = [d_1, \cdots, d_{N_{\text{r}}}]^T$ is the data vector for all users with covariance matrix

$$\boldsymbol{C_d} = \boldsymbol{I} . \tag{9}$$

The broadcast signal for VLC MU-MISO is generated through linear precoding of the data vector with the matrix $\boldsymbol{W}$, i.e.,

$$\boldsymbol{s} = [s_1, \ldots, s_{N_{\text{t}}}]^T = \boldsymbol{W}\boldsymbol{d} . \tag{10}$$

Finally, the transmitted current signal is given as

$$\boldsymbol{x} = \boldsymbol{W}\boldsymbol{d} + \boldsymbol{I}_{\text{DC}} . \tag{11}$$

We note that the conversion to a current signal and the scaling of the binary data vector $\boldsymbol{d}$ is accomplished through matrix $\boldsymbol{W}$. Hence, chosing $d_k \in \{\pm 1\}$ is without loss of generality. Furthermore, in VLC transmission, the elements of $\boldsymbol{x}$ must be non-negative, which imposes constraints on $\boldsymbol{W}$ as we will discuss further below.

Collecting the channel gains h_{kn} from (1) for all $N_{\text{r}} \times N_{\text{t}}$ links into the channel matrix $\boldsymbol{H} = [\boldsymbol{h}_1, \ldots, \boldsymbol{h}_{N_{\text{r}}}]^T = \{h_{kn}\}_{N_{\text{r}} \times N_{\text{t}}}$, the received signal at the k_{th} user can be written as

$$\begin{aligned} \hat{y}_k &= \boldsymbol{h}_k^T \boldsymbol{x} + z_k \\ &= \boldsymbol{h}_k^T \mathbf{w}_k d_k + \boldsymbol{h}_k^T \sum_{i \neq k} \mathbf{w}_i d_i + z_k + \boldsymbol{h}_k^T \boldsymbol{I}_{\text{DC}} , \end{aligned} \tag{12}$$

where $\mathbf{w}_k$ represents the k_{th} column of $\boldsymbol{W}$. The first term $\boldsymbol{h}_k^T \mathbf{w}_k d_k$ is the desired signal, while the second term $\boldsymbol{h}_k^T \sum_{i \neq k} \mathbf{w}_i d_i$ represents the intra-CoMP-attocell interference. The third term z_k is the sum of inter-CoMP-attocell interference and noise as introduced in (5). The fourth term $\boldsymbol{h}_k^T \boldsymbol{I}_{\text{DC}}$ is the DC photocurrent for illumination that carries no data. It is removed via AC coupling at the receiver side, providing the information-carrying signal at the k_{th} receiver as

$$y_k = \hat{y}_k - \boldsymbol{h}_k^T \boldsymbol{I}_{\text{DC}} = \boldsymbol{h}_k^T \mathbf{w}_k d_k + \boldsymbol{h}_k^T \sum_{i \neq k} \mathbf{w}_i d_i + z_k . \tag{13}$$

C. Constraints on Precoding from VLC

Consider the precoding operation in (10), the data signal s_n at the n_{th} luminary satisfies

$$-\|\boldsymbol{w}_n\|_1 \leq s_n \leq \|\boldsymbol{w}_n\|_1, \tag{14}$$

where $\boldsymbol{w}_n$ is the n_{th} row vector of the precoding matrix $\boldsymbol{W}$. After adding the DC bias, I_{DC}^n, to adjust the brightness of each LED luminary, the electrical transmit signal (drive current) at the n_{th} LED luminary is (see (11))

$$x_n = s_n + I_{\text{DC}}^n . \tag{15}$$

For simplicity, in the following we assume the same brightness level for every LED luminary, i.e.,

$$I_{\text{DC}}^n = I_{\text{DC}} , \quad \forall n . \tag{16}$$

Due to optical intensity modulation, $x_n \geq 0$ and thus $s_n \geq -I_{\text{DC}}$ from (15). However, similar to the nonlinearity of RF transmitters, LEDs also have a limited linear range [23]. While pre-distortion can be used to (approximately) linearize transmission, signal clipping needs to be avoided.

[1] Higher-order pulse-amplitude modulation schemes could also be employed in the case of high SINRs at the receivers. The precoder design would follow a similar approach as shown here for OOK.

Furthermore, if the LED is over-driven, not only will LED life-expectancy be reduced, but the self-heating effect will lead to a drop in the electrical-to-optical conversion efficiency. Considering these characteristics of LEDs, the transmit signal of each LED luminary should satisfy

$$I_{\mathrm{L}} \leq x_n = s_n + I_{\mathrm{DC}} \leq I_{\mathrm{U}} \ , \tag{17}$$

where $I_{\mathrm{U}} > I_{\mathrm{L}} > 0$ represent the upper and the lower bound of the LED drive current in the linear region. Substituting this into (14), we get

$$\begin{aligned} I_{\mathrm{DC}} - \|\boldsymbol{w}_n\|_1 &\geq I_{\mathrm{L}} \\ I_{\mathrm{DC}} + \|\boldsymbol{w}_n\|_1 &\leq I_{\mathrm{U}} \end{aligned} \tag{18}$$

and the constraint

$$\|\boldsymbol{w}_n\|_1 \leq \min\left(I_{\mathrm{DC}} - I_{\mathrm{L}}, I_{\mathrm{U}} - I_{\mathrm{DC}}\right) \tag{19}$$

for the n_{th} row vector of the precoder matrix $\boldsymbol{W}$. Note that, via I_{DC}, this constraint ties possible choices of VLC precoding matrices $\boldsymbol{W}$ to the user-selected illumination level of the LEDs.

D. Design Objectives

Given the broadcast transmission model (13) and constraint (19), we optimize the precoding represented by $\boldsymbol{W}$ in two ways. First, we consider the perhaps more obvious design task of maximizing the performance of MU-MISO VLC under illumination constraints, i.e., a given value of I_{DC}. As an appropriate performance measure for MU-MISO VLC we adopt the sum mean-square error (sum-MSE). Secondly, we consider a VLC performance target represented by a given set of MSE thresholds for all users, and find the minimal illumination level required to maintain performance. This design provides a guaranteed VLC performance under different dimming levels. The two design objectives are pursued in Section III, assuming that perfect CSI, i.e., channel gains h_{kn} (1), are available at the VLC transmitters. In Section IV, we extend our derivations to the practically relevant case of imperfect channel knowledge at the transmitter.

III. Precoder Design with Perfect CSI

As mentioned above, the performance metric for precoder design adopted in this work is the sum MSE, which has widely been considered for precoding optimization in RF wireless MIMO/MISO systems, e.g., [24]. In particular, we consider the modified MSE [25] between the received signal y_k at the k_{th} user and original data d_k given by

$$\begin{aligned} \mathrm{MSE}_k &= \mathbb{E}_{d_k,z_k}\left\{\|cy_k - d_k\|_2^2\right\} \\ &= \mathbb{E}_{\boldsymbol{d},z_k}\{\|c(\boldsymbol{h}_k^T\boldsymbol{W}\boldsymbol{d} + z_k) - \boldsymbol{e}_k^T\boldsymbol{d}\|_2^2\} \ , \end{aligned} \tag{20}$$

where c is a scaling term, which does not need to be applied at the receiver but offers a required degree of freedom in the receiver filter optimization, and $\boldsymbol{e}_k$ denotes the k_{th} standard basis vector for the N_{r}-dimensional space,

$$\boldsymbol{e}_k = [\boldsymbol{0}_{1\times(k-1)} \ \ 1 \ \ \boldsymbol{0}_{1\times(N_{\mathrm{r}}-k)}]^T. \tag{21}$$

A. Sum-MSE Minimization Problem

We first consider the sum-MSE minimization under illumination constraints. In this case, the precoder optimization problem can be formulated as

$$\begin{aligned} \mathrm{P1}: (\boldsymbol{W}^*, c^*) &= \underset{\boldsymbol{W},c}{\operatorname{argmin}} \sum_{k=1}^{N_{\mathrm{r}}} \mathrm{MSE}_k \\ \mathrm{C1}: \|\boldsymbol{w}_n\|_1 &\leq \min\left(I_{\mathrm{DC}} - I_{\mathrm{L}}, I_{\mathrm{U}} - I_{\mathrm{DC}}\right), \forall n \end{aligned} \tag{22}$$

Using (20), the objective function in P1 can be written as

$$f(\boldsymbol{W}, c) = \sum_{k=1}^{N_{\mathrm{r}}} \mathrm{MSE}_k = \mathbb{E}_{\boldsymbol{d},\boldsymbol{z}}\left\{\|c\boldsymbol{y} - \boldsymbol{d}\|_2^2\right\} \ . \tag{23}$$

The optimization problem P1 is not jointly convex in precoder $\boldsymbol{W}$ and scaling factor c. We therefore use an alternating optimization approach to, possibly suboptimally, solve this problem. Specifically, we iteratively optimize $\boldsymbol{W}$ and c while fixing the other variable.

1) Fixing Receiver Gain c: We assume a fixed receiver gain c and then optimize the precoder $\boldsymbol{W}$. In this case, it is convenient to define

$$\sigma_{\mathrm{sum}}^2 = \sum_{k=1}^{N_{\mathrm{r}}} \sigma_k^2 \tag{24}$$

and to write the sum-MSE as

$$\begin{aligned} \mathbb{E}_{\boldsymbol{d},\boldsymbol{z}}\left\{\|c\boldsymbol{y} - \boldsymbol{d}\|_2^2\right\} &= \mathbb{E}_{\boldsymbol{d},\boldsymbol{n}}\left\{\|c(\boldsymbol{H}\boldsymbol{W}\boldsymbol{d} + \boldsymbol{z}) - \boldsymbol{d}\|_2^2\right\} \\ &= \|c(\boldsymbol{H}\otimes\boldsymbol{I})\mathrm{vec}(\boldsymbol{W}^T) - \mathrm{vec}(\boldsymbol{I})\|_2^2 + c^2\sigma_{\mathrm{sum}}^2 \end{aligned} \tag{25}$$

Then, defining $\boldsymbol{b} = \mathrm{vec}(\boldsymbol{I})$, $\boldsymbol{A} = \boldsymbol{H}\otimes\boldsymbol{I}$, $\boldsymbol{w} = \mathrm{vec}(\boldsymbol{W}^T)$, and $\boldsymbol{V}$ as the $N_{\mathrm{t}}N_{\mathrm{r}} \times N_{\mathrm{t}}N_{\mathrm{r}}$ block-diagonal matrix of the $N_{\mathrm{t}} \times N_{\mathrm{r}}$ all-one matrix, problem P1, for a fixed gain c, can be transformed into

$$\begin{aligned} \mathrm{P2}: (\boldsymbol{w}^*, \boldsymbol{t}^*) &= \underset{\boldsymbol{w},\boldsymbol{t}}{\operatorname{argmin}} \|c\boldsymbol{A}\boldsymbol{w} - \boldsymbol{b}\|_2^2 + c^2\sigma_{\mathrm{sum}}^2 \\ \mathrm{C1}: -\boldsymbol{t} &\leq \boldsymbol{w} \leq \boldsymbol{t} \\ \mathrm{C2}: \boldsymbol{V}\boldsymbol{t} &\leq \min\left(I_{\mathrm{DC}} - I_{\mathrm{L}}, I_{\mathrm{U}} - I_{\mathrm{DC}}\right)\boldsymbol{1}_{N_{\mathrm{r}}\times 1} \end{aligned} \tag{26}$$

where $\boldsymbol{t}$ is a slack variable. The constraints in this optimization problem are equivalent to the L_1-norm constraint (19) resulting from the limited dynamic range of the LED. This problem is a convex quadratic programming problem and can be efficiently solved using, e.g., YALMIP or CVX toolbox [26], [27].

2) Fixing Precoder $\boldsymbol{W}$: Now we assume the precoder matrix $\boldsymbol{W}$ as fixed and optimize for c. The optimization problem P1 with fixed precoder $\boldsymbol{W}$ can be simplified into

$$\mathrm{P3}: c^* = \underset{\boldsymbol{c}}{\operatorname{argmin}} \|c\boldsymbol{A}\boldsymbol{w} - \boldsymbol{b}\|_2^2 + c^2\sigma_{\mathrm{sum}}^2 \ .$$

The optimal c^* can now be computed as

$$c^* = \frac{\mathrm{sym}(\boldsymbol{b}^{\boldsymbol{T}}\boldsymbol{A}\boldsymbol{w})}{\|\boldsymbol{A}\boldsymbol{w}\|_2^2 + \sigma_{\mathrm{sum}}^2} \ , \tag{27}$$

where

$$\mathrm{sym}(\boldsymbol{X}) = \frac{\boldsymbol{X} + \boldsymbol{X}^{\boldsymbol{T}}}{2} \tag{28}$$

represents the symmetric part of a matrix $\boldsymbol{X}$.

B. Minimal Illumination Level Problem

We now turn to the question of what is the minimal illumination level needed to maintain a certain VLC performance, termed here as the "minimal illumination level problem" in this paper. This is important for illumination systems with dimming, for which VLC should be supported. Illumination is proportional to I_{DC}, which via (19) affects VLC precoding. Measuring VLC performance in terms of MSE and denoting by q_k the constraint for the MSE of the k_{th} user, the corresponding optimization problem can be formulated as

$$\begin{aligned} \mathrm{P4}: (\boldsymbol{W}^*, c^*, I_{\mathrm{DC}}^*) = &\underset{\boldsymbol{W},c,I_{\mathrm{DC}}}{\operatorname{argmin}} \; I_{\mathrm{DC}} \\ &\mathrm{C1}: \mathrm{MSE}_k \leq q_k, \forall k \\ &\mathrm{C2}: \|\boldsymbol{w}_n\|_1 \leq \min\left(I_{\mathrm{DC}} - I_{\mathrm{L}}, I_{\mathrm{U}} - I_{\mathrm{DC}}\right), \forall n \end{aligned} \tag{29}$$

Writing

$$\mathrm{MSE}_k = (c\boldsymbol{h}_k^T\boldsymbol{W} - \boldsymbol{e}_k^T)(c\boldsymbol{h}_k^T\boldsymbol{W} - \boldsymbol{e}_k^T)^T + c^2\sigma_k^2 \tag{30}$$

and defining

$$\begin{aligned} \zeta &= 1/c, \\ \boldsymbol{v}_k^T &= (\boldsymbol{h}_k^T\boldsymbol{W} - \zeta\boldsymbol{e}_{\boldsymbol{k}}^{\boldsymbol{T}}), \\ \boldsymbol{\phi}_k &= [\boldsymbol{v}_k^T \quad \sigma_k], \end{aligned} \tag{31}$$

the constraint $\mathrm{MSE}_k \leq q_k$ can be expressed as

$$\|\boldsymbol{\phi}_k\|_2 \leq \sqrt{q_k}\zeta \; . \tag{32}$$

According to the Schur complement lemma [28][29], inequality (32) is equivalent to

$$\boldsymbol{\Theta}_k = \begin{bmatrix} \sqrt{q_k}\zeta & \boldsymbol{\phi}_k \\ \boldsymbol{\phi}_k^T & \sqrt{q_k}\zeta\boldsymbol{I} \end{bmatrix} \succeq 0 \; .$$

Thus, P4 can be reformulated as

$$\begin{aligned} \mathrm{P5}: (\boldsymbol{W}^*, \zeta^*, I_{\mathrm{DC}}^*) = &\underset{\boldsymbol{W},\{\boldsymbol{t}_k\},\zeta,I_{\mathrm{DC}}}{\operatorname{argmin}} \quad I_{\mathrm{DC}} \\ &\mathrm{C1}: -\boldsymbol{t}_k \leq \boldsymbol{W}^T\boldsymbol{e}_k \leq \boldsymbol{t}_k, \forall k \\ &\mathrm{C2}: \mathbf{1}^T\boldsymbol{t}_k \leq \min\left(I_{\mathrm{DC}} - I_{\mathrm{L}}, I_{\mathrm{U}} - I_{\mathrm{DC}}\right), \forall k \\ &\mathrm{C3}: \boldsymbol{\Theta}_k \succeq 0, \forall k \end{aligned} \tag{33}$$

where vector $\boldsymbol{t}_k$ is a slack variable. The problem is a convex semidefinite programming problem (SDP) and can be solved efficiently numerically, e.g., [26], [27].

IV. Precoder Design with Channel Uncertainty

The quality of CSI at the transmitter is critical to the precoder design. While the VLC channel is much more benign than its RF counterpart, the assumption of perfect CSI is not necessarily practical for MU-MISO VLC. VLC systems use visible light as the downlink medium, while the uplink medium can be RF, infrared light (IR) or visible light [30]. In the case of VLC uplink, the uplink-downlink reciprocity will allow CSI to be estimated at the transmitter. The more practically relevant scenario for VLC using indoor illumination devices considered here is that an RF uplink is used. In this case, CSI can only be estimated at the receiver and fed back to the transmitter afterwards. Imperfect CSI can then arise from noisy and quantized channel estimation and, perhaps more critically, the feedback of outdated estimates. The latter is the case when the VLC channel varies due to terminal motion and/or changes in the environment since the last channel update. As an example, Figure 2 illustrates a scenario where the receiver terminal has moved from position $\boldsymbol{p}_1$, at which CSI is reported, to position $\boldsymbol{p}_2$, at which precoded data using this CSI is received.

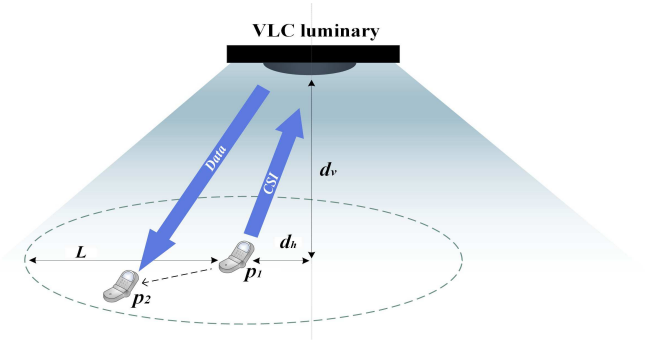

Figure 2: Illustration of outdated CSI resulting from terminal mobility in a VLC system.

A. Uncertainty Models

Given the channel estimate $\hat{\boldsymbol{h}}_k$, we can express the true channel gains for the k_{th} user as

$$\boldsymbol{h}_k = \hat{\boldsymbol{h}}_k + \boldsymbol{\delta}_k \; , \tag{34}$$

where the error vector $\boldsymbol{\delta}_k$ represents the CSI uncertainty. According to the source of estimation error, we consider two models for $\boldsymbol{\delta}_k$.

1) Noisy CSI: For noisy CSI, we use the stochastic error model [28]

$$\boldsymbol{\delta}_k \sim \mathcal{N}(0, \boldsymbol{\Sigma}_k) \; , \tag{35}$$

i.e., $\boldsymbol{\delta}_k$ is zero-mean Gaussian distributed with covariance matrix $\boldsymbol{\Sigma}_k$.

2) Outdated CSI: Outdated CSI, due to e.g. a user walking with a terminal device (see Figure 2), is often modelled by a bounded uncertainty model, i.e.,

$$\|\boldsymbol{\delta}_k\|_2 \leq \epsilon_k \tag{36}$$

for some error bound ϵ_k, which depends on the maximal changes that happened between CSI estimation and transmission using this estimation. As we show in the following, ϵ_k should be chosen as a function of the terminal location during channel estimation, i.e., $\boldsymbol{p}_1$ in Figure 2. Location information could be obtained from channel estimation itself using various positioning techniques [31], [32].

Referring to Figure 2, we denote L as the bound for the user movement between two CSI updates, i.e., $\|\boldsymbol{p}_1 - \boldsymbol{p}_2\|_2 \leq L$. Furthermore, considering a single transmitter, let d_v and d_h be the vertical and horizontal distance between transmitter and receiver, respectively, as indicated in Figure 2. Then, for terminal movement in horizontal direction, horizontal planes at the LED transmitter and photodiode receiver, and constant optical filter gain $T(\psi_{kn_i}) = T_k$, the error bound

$$\epsilon_k = \max\{\epsilon_+, \epsilon_-\} \tag{37}$$

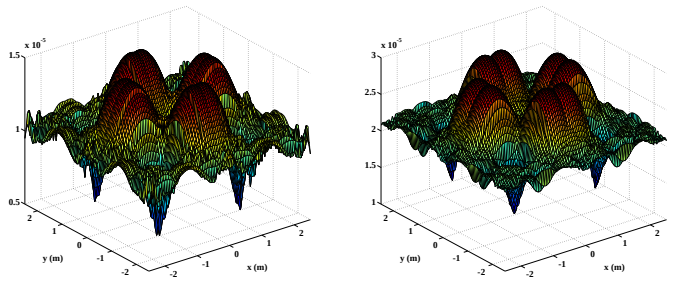

(a) (b)

Figure 3: Error bounds obtained from simulation for $(a): L = 0.25$ m, $(b): L = 0.5$ m. Illumination and VLC setup for these results are described in Section V.

can be obtained, where

$$\epsilon_+ = \beta\left((d_v^2+d_1^2)^{-\frac{m+3}{2}} - (d_v^2+(d_1+L)^2)^{-\frac{m+3}{2}}\right), \quad (38)$$

$$\epsilon_- = \beta\left((d_v^2+(d_2-L)^2)^{-\frac{m+3}{2}} - (d_v^2+d_2^2)^{-\frac{m+3}{2}}\right), \quad (39)$$

$$\beta = \frac{(m+1)KA_kT_kG_kd_v^{m+1}}{2\pi}, \quad (40)$$

and d_1 and d_2 satisfy

$$\log\left(\frac{d_1}{d_1+L}\right) = \frac{m+5}{2}\log\left(\frac{d_v^2+d_1^2}{d_v^2+(d_1+L)^2}\right), \quad (41)$$

$$\log\left(\frac{d_2}{d_2-L}\right) = \frac{m+5}{2}\log\left(\frac{d_v^2+d_2^2}{d_v^2+(d_2-L)^2}\right). \quad (42)$$

For the more general case including multiple transmitters, the relationship between error bound and physical system parameters is even more complicated than (37). We thus resort to numerical analysis to obtain error bounds. As an example, Figure 3 shows ϵ_k as function of the user location and the maximal location distance L. The details for the room, illumination and VLC setup for this experiment are described in Section V.

In the following, we consider both uncertainty models to formulate robust precoder designs. Similar to the RF wireless case, cf. e.g. [28], [29], we aim at optimizing average performance for noisy CSI according to the stochastic model (35) and worst-case performance for outdated CSI with the bounded error model (36).

B. Sum-MSE Minimization Problem

We start with the sum-MSE minimization problem.

1) Robust Design with Outdated CSI: The robust broadcast precoder design for CSI uncertainty according to (36) is an extension of P1 in (22):

$$\begin{aligned}\text{P6}: (\boldsymbol{W}^*, c^*) &= \underset{\boldsymbol{W},c}{\operatorname{argmin}} \max_{\|\boldsymbol{\delta_k}\|_2\le\epsilon_k} \sum_{k=1}^{N_\text{r}} \text{MSE}_k \\ \text{C1}: \|\boldsymbol{w}_n\|_1 &\le \min\left(I_\text{DC}-I_\text{L}, I_\text{U}-I_\text{DC}\right), \forall n \end{aligned} \quad (43)$$

where

$$\text{MSE}_k = \|c(\hat{\boldsymbol{h}}_k^T + \boldsymbol{\delta}_k^T)\boldsymbol{W} - \boldsymbol{e}_k^T\|_2^2 + c^2\sigma_k^2. \quad (44)$$

Using results from [28], P6 can be transformed into

$$\begin{aligned}\text{P7}: (\boldsymbol{W}^*, c^*) &= \underset{\boldsymbol{W},\{\boldsymbol{t}_k\},\boldsymbol{\lambda},\boldsymbol{\mu},g,c}{\operatorname{argmin}} \quad g^2 \\ \text{C1}&: -\boldsymbol{t}_k \le \boldsymbol{W}^T\boldsymbol{e}_k \le \boldsymbol{t}_k, \forall k \\ \text{C2}&: \mathbf{1}^T\boldsymbol{t}_k \le \min\left(I_\text{DC}-I_\text{L}, I_\text{U}-I_\text{DC}\right), \forall k \\ \text{C3}&: \boldsymbol{\Psi_k} \succeq \mathbf{0}, \forall k \\ \text{C4}&: \boldsymbol{\Phi} \succeq \mathbf{0} \end{aligned} \quad (45)$$

where

$$\boldsymbol{\Phi} = \begin{bmatrix} g & \boldsymbol{\lambda}^T & c\sigma_\text{sum} \\ \boldsymbol{\lambda} & g\boldsymbol{I} & \mathbf{0} \\ c\sigma_\text{sum} & \mathbf{0} & g \end{bmatrix}$$

$$\boldsymbol{\Psi}_k = \begin{bmatrix} \lambda_k-\mu_k & \mathbf{0}^T & c\hat{\boldsymbol{h}}_k^T\boldsymbol{W} - \boldsymbol{e}_k^T \\ \mathbf{0} & \mu_k\boldsymbol{I} & \epsilon_k c\boldsymbol{W} \\ (c\hat{\boldsymbol{h}}_k^T\boldsymbol{W} - \boldsymbol{e}_k^T)^T & \epsilon_k(c\boldsymbol{W})^T & \lambda_k\boldsymbol{I} \end{bmatrix}$$

Similar to the optimization problem P1, we can obtain a local optimum of this problem by alternatively optimizing over $\boldsymbol{W}$ and c. Each problem is an SDP problem and can be efficiently solved numerically, e.g., [26], [27].

2) Robust Design with Noisy CSI: As noted above, the average sum-MSE is considered. Defining

$$\boldsymbol{\Delta} = [\boldsymbol{\delta}_1, \ldots, \boldsymbol{\delta}_{N_\text{r}}]^T, \quad (46)$$

the optimization problem can be formulated as

$$\begin{aligned}\text{P8}: (\boldsymbol{W}^*, c^*) &= \arg\min_{\boldsymbol{W},c} \mathbb{E}_{\boldsymbol{\Delta}}\left(\sum_{k=1}^{N_\text{r}} \text{MSE}_k\right) \\ \text{C1}&: \|\boldsymbol{w}_n\|_1 \le \min\left(I_\text{DC}-I_\text{L}, I_\text{U}-I_\text{DC}\right), \forall n \end{aligned} \quad (47)$$

Following the steps in (23) and (25) and assuming $\boldsymbol{\Sigma}_k = \sigma_e^2\boldsymbol{I}$, we can write the objective of P8 as

$$\mathbb{E}_{\boldsymbol{\Delta}}\left(f(\boldsymbol{W},c)\right) = (\|c\hat{\boldsymbol{A}}\boldsymbol{w} - \boldsymbol{b}\|_2^2 + N_\text{r}\sigma_e^2c^2\|\boldsymbol{w}\|_2^2) + c^2\sigma_\text{sum}^2, \quad (48)$$

where $\hat{\boldsymbol{A}} = \hat{\boldsymbol{H}} \otimes \boldsymbol{I}$, and $\hat{\boldsymbol{H}}$ is the estimated channel matrix. While P8 is not a convex optimization problem, again the application of alternating optimization for $\boldsymbol{W}$ and c turns out to be a suitable approach. When fixing the receiver gain c, we can optimize for $\boldsymbol{W}$ via

$$\begin{aligned}&\text{P9}: (\boldsymbol{w}^*, \boldsymbol{t}^*) \\ &= \underset{\boldsymbol{w},\boldsymbol{t}}{\operatorname{argmin}}(\|c\hat{\boldsymbol{A}}\boldsymbol{w} - \boldsymbol{b}\|_2^2 + N_\text{r}\sigma_e^2c^2\|\boldsymbol{w}\|_2^2) + c^2\sigma_\text{sum}^2 \\ &\text{C1}: -\boldsymbol{t} \le \boldsymbol{w} \le \boldsymbol{t} \\ &\text{C2}: \boldsymbol{V}\boldsymbol{t} \le \min\left(I_\text{DC}-I_\text{L}, I_\text{U}-I_\text{DC}\right)\mathbf{1}_{N_\text{r}\times 1} \end{aligned} \quad (49)$$

This problem is a convex quadratic programming problem, which is solved numerically. Fixing the precoder $\boldsymbol{W}$ leads to the closed-form solution

$$\begin{aligned}c^* &= \underset{c}{\operatorname{argmin}}\{\|c\hat{\boldsymbol{A}}\boldsymbol{w} - \boldsymbol{b}\|_2^2 + N_\text{r}\sigma_e^2c^2\|\boldsymbol{w}\|_2^2\} + c^2\sigma_\text{sum}^2 \\ &= \frac{\text{sym}(\boldsymbol{b^T}\hat{\boldsymbol{A}}\boldsymbol{w})}{\|\hat{\boldsymbol{A}}\boldsymbol{w}\|_2^2 + N_\text{r}\sigma_e^2\|\boldsymbol{w}\|_2^2 + \sigma_\text{sum}^2}. \end{aligned} \quad (50)$$

C. Minimal Illumination Level Problem

We finally turn to the robust design for minimizing the required illumination level for a given VLC performance.

1) Robust Design with Outdated CSI: To add robustness to the precoder design for minimal required brightness when CSI is outdated, the worst-case MSE needs to satisfy the required performance q_k:

$$\max_{\|\boldsymbol{\delta}_k\|_2 \leq \epsilon_k} \mathrm{MSE}_k \leq q_k, \forall k \tag{51}$$

Making use of the Schur complement lemma [28][29] and [33, Lemma 2], (51) is equivalent to $\exists\ \lambda_k \geq 0$,

$$\boldsymbol{\Psi}_k = \begin{bmatrix} \sqrt{q_k}\zeta - \lambda_k & \hat{\boldsymbol{v}}_k^T & \sigma_k & \mathbf{0} \\ \hat{\boldsymbol{v}}_k & \sqrt{q_k}\zeta \boldsymbol{I} & \mathbf{0} & -\epsilon_k \boldsymbol{W}^T \\ \sigma_k & \mathbf{0} & \sqrt{q_k}\zeta & \mathbf{0} \\ \mathbf{0} & -\epsilon_k \boldsymbol{W} & \mathbf{0} & \lambda_k \boldsymbol{I} \end{bmatrix} \succeq \mathbf{0},$$

where

$$\hat{\boldsymbol{v}}_{\boldsymbol{k}}^{\boldsymbol{T}} = (\hat{\boldsymbol{h}}_{\boldsymbol{k}}^{\boldsymbol{T}} \boldsymbol{W} - \zeta \boldsymbol{e}_{\boldsymbol{k}}^{\boldsymbol{T}}) \,. \tag{52}$$

Hence, we obtain the optimization problem

$$\begin{aligned} \mathrm{P10}: (\boldsymbol{W}^*, \zeta^*, I_{\mathrm{DC}}^*) = & \underset{\boldsymbol{W}, \boldsymbol{\lambda}, \zeta, I_{\mathrm{DC}}}{\operatorname{argmin}} \ I_{\mathrm{DC}} \\ & \mathrm{C1}: -\boldsymbol{t}_k \leq \boldsymbol{W}^T \boldsymbol{e}_k \leq \boldsymbol{t}_k, \forall k \\ & \mathrm{C2}: \mathbf{1}^T \boldsymbol{t}_k \leq \min\left(I_{\mathrm{DC}} - I_{\mathrm{L}}, I_{\mathrm{U}} - I_{\mathrm{DC}}\right), \forall k \\ & \mathrm{C3}: \boldsymbol{\Psi}_k \succeq \mathbf{0}, \forall k \\ & \mathrm{C4}: \lambda_k \geq 0, \forall k \end{aligned} \tag{53}$$

This problem is an SDP and the global optimum can be obtained on condition that it is feasible.

2) Robust Design with Noisy CSI: In the case of noisy CSI, we need to replace C1 in P4 (29) by

$$\mathbb{E}_{\boldsymbol{\delta}_k}(\mathrm{MSE}_k) = c^2 \hat{\boldsymbol{v}}_k^T \hat{\boldsymbol{v}}_k + c^2 \sigma_e^2 \|\boldsymbol{W}\|_F^2 + c^2 \sigma_k^2 \,. \tag{54}$$

Introducing auxiliary variable r and $\boldsymbol{\tau}_k = [\hat{\boldsymbol{v}}_k^T \quad r \quad \sigma_k]$, $\mathbb{E}_{\boldsymbol{\delta}_k}(\mathrm{MSE}_k) \leq q_k$ becomes equivalent to

$$\begin{aligned} \|\boldsymbol{\tau}_k\|_2 &\leq \sqrt{q_k}\zeta \\ \|\boldsymbol{W}\|_F &\leq \frac{r}{\sigma_e} \end{aligned} \tag{55}$$

Therefore, we can formulate the precoder design problem as

$$\begin{aligned} \mathrm{P11}: (\boldsymbol{W}^*, \zeta^*, I_{\mathrm{DC}}^*) = & \underset{\boldsymbol{W}, \{\boldsymbol{t}_k\}, \{\boldsymbol{\tau}_k\}, \zeta, r, I_{\mathrm{DC}}}{\operatorname{argmin}} \ I_{\mathrm{DC}} \\ & \mathrm{C1}: -\boldsymbol{t}_k \leq \boldsymbol{W}^T \boldsymbol{e}_k \leq \boldsymbol{t}_k, \forall k \\ & \mathrm{C2}: \mathbf{1}^T \boldsymbol{t}_k \leq \min\left(I_{\mathrm{DC}} - I_{\mathrm{L}}, I_{\mathrm{U}} - I_{\mathrm{DC}}\right), \forall k \\ & \mathrm{C3}: \|\boldsymbol{W}\|_F \leq \frac{r}{\sigma_e} \\ & \mathrm{C4}: \boldsymbol{\Upsilon}_k \succeq 0, \forall k \end{aligned} \tag{56}$$

where

$$\boldsymbol{\Upsilon}_k = \begin{bmatrix} \sqrt{q_k}\zeta & \boldsymbol{\tau}_k \\ \boldsymbol{\tau}_k^T & \sqrt{q_k}\zeta \boldsymbol{I} \end{bmatrix} \,.$$

This problem is again an SDP.

V. Numerical Results and Discussions

In this section, we present and discuss the simulation results for the proposed MU-MISO VLC system assuming different coordination levels, user positions, interference levels and channel uncertainty scenarios in an indoor environment. We consider an example setup of a room with $N_{\mathrm{t}} = 4$ coordinated and VLC-enabled LED luminaries at the ceiling. Room dimensions and luminary locations are listed in Table I. The table also summarizes the luminary and LED parameters, where the latter apply to LXW8-PW40 Luxeon Rebel high power LEDs [34]. The illuminance level when $I_{\mathrm{DC}} = 500$ mA, i.e., $I_{\mathrm{DC}} = (I_{\mathrm{L}} + I_{\mathrm{U}})/2$, with this system setup is shown in Figure 4. According to [35], the illuminance level and uniformity (0.645 in this case) is sufficient for office work and study. The background current of $I_{\mathrm{bg}} = 100$ μA accounts for ambient light from other sources such as sunlight or non-VLC enabled luminaries, and the thermal noise is considered negligible. We confirmed via measurements that these are valid assumptions.[2]

Table I: Simulation parameters.

Room Setup	
Fixture coordinate 1	[1.25, 1.25, 3]
Fixture coordinate 2	[1.25, -1.25, 3]
Fixture coordinate 3	[-1.25, -1.25, 3]
Fixture coordinate 4	[-1.25, 1.25, 3]
Room Length L × W × H	5 [m] × 5 [m] × 3 [m]

Transmitter Parameters	
I_{L}	400 [mA]
I_{U}	600 [mA]
Semi-angle at half power $\phi_{\frac{1}{2}}$	60 [deg.]
Dimensions of LED L × W × H	3 [cm]×3 [cm]×2 [cm]
LED interval	1 [cm]
Number of LEDs per luminary K	36 (6×6)

Receiver Parameters	
PD area	1 cm^2
Refractive index of optical concentrator κ	1.5
Gain of optical filter	1
Receiver FOV	60 [deg.]
System bandwidth B	10 [MHz]
Noise bandwidth factor I_2	0.562
Background current I_{bg}	100 [μA]
LED conversion factor s	0.44 [W/A]
PD responsivity γ	0.30 [A/W]

In the following, we assume that the VLC system transmits to $N_{\mathrm{r}} = 4$ users. For concreteness, we further assume that the four users are centro-symmetrically located on the plane at height $z = 0.8$ m, i.e., the user coordinates are $(\pm x, \pm y, 0.8)$ m for some x and y. We would like to emphasize that the specific system parameters, in particular the values of N_{t} and N_{r}, are chosen for the sake of illustration of precoded transmission only, and that our system design approach is applicable to any parameter pair $(N_{\mathrm{t}}, N_{\mathrm{r}})$.

In the subsequent sections, we report performance results for different transmission scenarios and precoder designs. Due to symmetry, the performance for the $N_{\mathrm{r}} = 4$ users are

[2]We also ran simulations assuming larger I_{bg} values of 620 μA [36] and even 5 mA [20], where especially the latter can be considered as an extreme worst-case noise scenario. We found however that the main trends of our results as discussed in the following are not affected by the value of the background current.

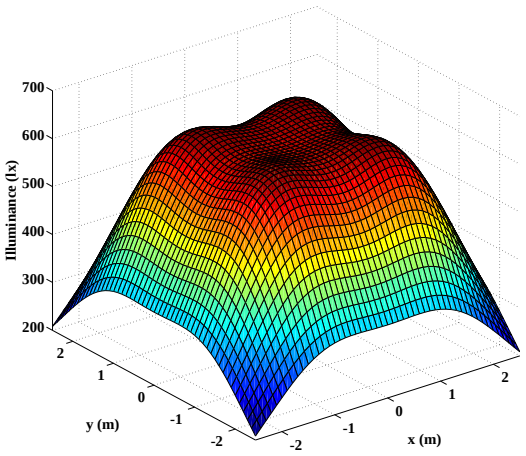

Figure 4: The distribution of indoor luminance when $I_{\mathrm{DC}} = 500$ mA.

identical, and thus we can drop the user index for the results. If not stated otherwise, perfect CSI for the precoder design is assumed. For solving the convex optimization problems in this paper, we use the YALMIP toolbox [26] in conjunction with the MOSEK solver [37] to obtain the result numerically. For solving the sum-MSE minimization problems via alternating optimization, the zero-forcing solution is used for initialization and the maximum number of iterations is set to 20.

A. User Position with Full Coordination Setup

We first investigate the achievable performance for a VLC broadcast system where LED luminaries are fully connected by a PLC backbone network and coordinated by a PLC controller. The users are arranged in three different setups as shown in the first three arrangements in Fig. 5, where $x = y = 0.5$ in Setup I, $x = y = 1.25$ in Setup II and $x = y = 2$ in Setup III, respectively. The channel matrices for these three setups are obtained as

$$\boldsymbol{H}_{\mathrm{I}} = 10^{-5} \begin{bmatrix} 6.164 & 3.067 & 1.829 & 3.067 \\ 3.067 & 6.164 & 3.067 & 1.829 \\ 1.829 & 3.067 & 6.164 & 3.067 \\ 3.067 & 1.829 & 3.067 & 6.164 \end{bmatrix}$$

$$\boldsymbol{H}_{\mathrm{II}} = 10^{-5} \begin{bmatrix} 9.340 & 1.788 & 0.731 & 1.788 \\ 1.788 & 9.340 & 1.788 & 0.731 \\ 0.731 & 1.788 & 9.340 & 1.788 \\ 1.788 & 0.731 & 1.788 & 9.340 \end{bmatrix}$$

$$\boldsymbol{H}_{\mathrm{III}} = 10^{-5} \begin{bmatrix} 6.164 & 0.863 & 0.000 & 0.863 \\ 0.863 & 6.164 & 0.863 & 0.000 \\ 0.000 & 0.863 & 6.164 & 0.863 \\ 0.863 & 0.000 & 0.863 & 6.164 \end{bmatrix}$$

Figure 6 shows the results of the sum-MSE minimization problem as a function of the DC bias I_{DC}, i.e., the illumination level, for the three user-configurations from Fig. 5. Here we use the resulting optimal precoder to calculate the corresponding SINR defined as

$$\mathrm{SINR} = \frac{\|\boldsymbol{h}_k^T \mathbf{w}_k\|_2^2}{\|\boldsymbol{h}_k^T \sum_{i \neq k} \mathbf{w}_i\|_2^2 + \sigma_k^2} \,. \tag{57}$$

First, we observe that the system performance is symmetric with respect to $I_{\mathrm{DC}} = (I_{\mathrm{L}} + I_{\mathrm{U}})/2$. The SINR first increases as the DC bias I_{DC} increases and then starts to decrease after I_{DC} surpasses $(I_{\mathrm{L}} + I_{\mathrm{U}})/2$. This is because the electrical SINRs at the receivers reach their maximal values when the precoded signal s_n has the largest dynamic range. Due to this symmetry property, we will only plot the results for I_{DC} ranging from I_{L} to $(I_{\mathrm{L}} + I_{\mathrm{U}})/2$ in the following figures. For varying positions of the four users, the setups in increasing order of SINR value are Setup I, Setup III and Setup II. An intuitive explanation is that since the users in Setup I are closer to each other than in Setup III, the channels are more similar and thus more difficult to separate through precoding. Meanwhile, the distances between the LED luminaries and users in Setup III are larger than those in Setup II, which leads to smaller channel gains in Setup III than in Setup II.

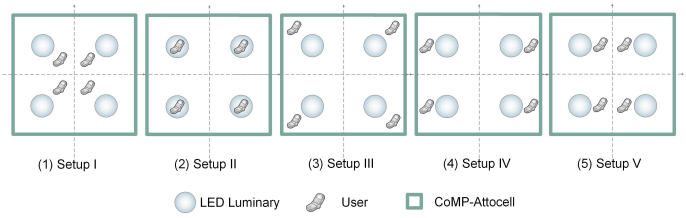

Figure 5: User-configurations for MU-MISO VLC are considered for numerical results.

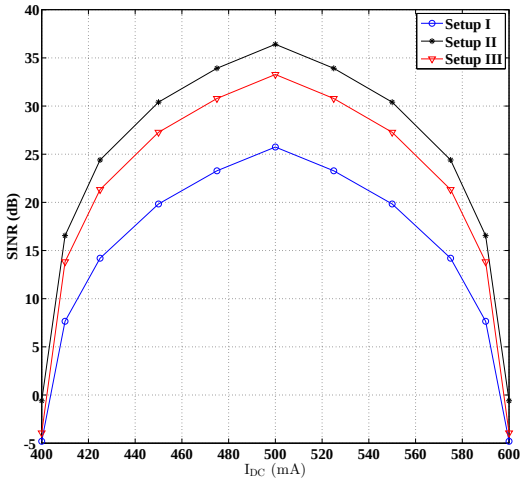

Figure 6: Comparison of system performance with different user positions (as shown in Fig. 5) as a function of illumination level. Sum-MSE minimization with perfect CSI.

B. Different Transmitter Coordination Level

We now highlight the benefit of coordination. Therefore, and only in this section, we compare systems with different values for N_{t} and N_{r}. More specifically, we consider three different coordination levels:

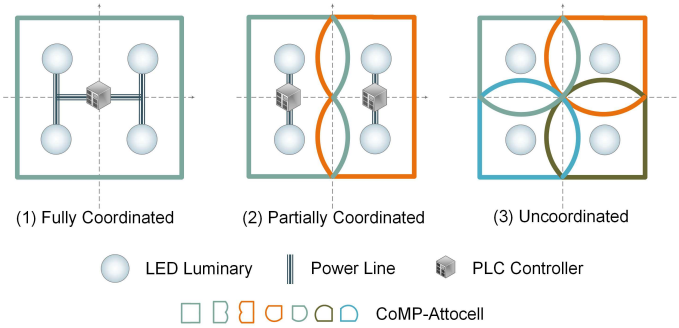

Figure 7: Different transmitter coordination levels in an MU-MISO VLC system.

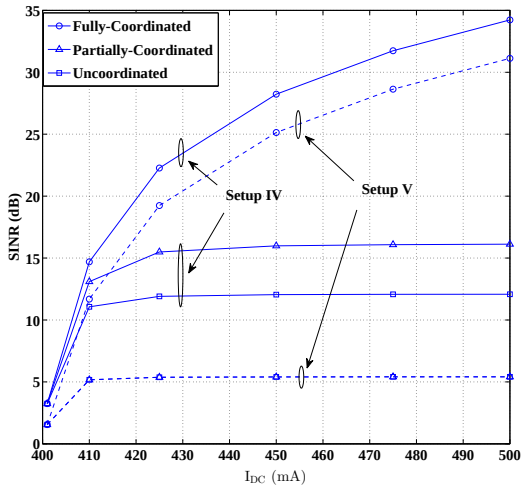

Figure 8: Comparison of system performance with different transmitter coordination. Sum-MSE minimization problem with perfect CSI.

1) *Fully coordinated (FC) system*: Transmissions for all four LED luminaries are coordinated, i.e., $N_{\mathrm{t}} = N_{\mathrm{r}} = 4$.
2) *Partially coordinated (PC) system*: Transmissions for LED luminaries in the first and the fourth quadrant and for LED luminaries in the second and the third quadrant are coordinated. Thus there exist two VLC CoMP-attocells in one room and for each of these systems $N_{\mathrm{t}} = N_{\mathrm{r}} = 2$ applies.
3) *Uncoordinated (UC) system*: Transmissions at the four LED luminaries are not coordinated, which corresponds to four VLC CoMP-attocells in one room. Each of these systems has parameters $N_{\mathrm{t}} = N_{\mathrm{r}} = 1$.

The three coordination levels are illustrated in Fig. 7.

We consider two scenarios for user locations: Setup IV with $x = 2$, $y = 1.25$ and Setup V with $x = 0.5$, $y = 1.25$ as shown in Fig. 5. Figure 8 shows the SINR for precoder design minimizing the sum-MSE as a function of I_{DC} for different coordination levels and user position scenarios. We observe that, since users are located closer to each other and/or the neighbouring CoMP-attocell boundary in Setup V than for Setup IV, the achievable SINR is generally higher for the latter. We can also see the significant SINR increase due to coordination. In particular, the FC setup is clearly outperforming the PC and UC systems, whose SINR saturates quickly due to inter-cell interference. For Setup V, there is no performance difference for UC and PC systems, which is due to the remaining large inter-CoMP-attocell interference in spite of the partial coordination. In the PC system, each VLC transmitter tends to mostly communicate to its closest receiver, which makes the PC system equivalent to a UC system.

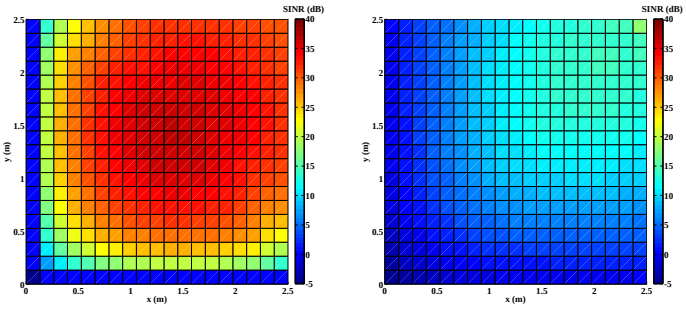

(a) FC system (b) UC system

Figure 9: SINR as a function of user location in one quadrant of the room and $I_{\mathrm{DC}} = (I_{\mathrm{L}} + I_{\mathrm{U}})/2$. Sum-MSE minimization problem with perfect CSI.

The benefit of (full) coordination is further demonstrated by the plots in Figure 9, which show the SINR for one quadrant of the room as a function of the user's location (because of the symmetry of the four user's location, the SINR plots for the other quadrants are mirrored versions of those in Figure 9) and for $I_{\mathrm{DC}} = (I_{\mathrm{L}} + I_{\mathrm{U}})/2$. It can be seen that the SINR is severely inter-attocell interference limited in the UC case, and that this problem can be overcome by coordination. In particular, the SINR for the FC system is uniformly high in almost the entire service area. Note that the lower SINR at the cell boundaries is an artifact of assuming centro-symmetrical user locations in our experiments, which means that at cell boundaries users are close to each other and thus interference is relatively high.

C. Sum-MSE Minimization with Channel Uncertainty

We now abandon the assumption of perfect CSI and consider channel uncertainty according to the models from Section IV-A. For the case of outdated CSI, we consider an assumed user location based on which we obtain a channel estimate $\hat{\boldsymbol{h}}_k$. Then, given a distance bound L, we obtain a CSI bound ϵ_k from numerical evaluation as shown in Section IV-A (see Fig. 3). Given $\hat{\boldsymbol{h}}_k$ and ϵ_k, the precoder $\boldsymbol{W}$ is obtained via P7 (45). Then, a set of actual channel gains $\boldsymbol{h}$ and associated SINRs (57) are generated by placing users uniformly at random into the uncertainty region. For the noisy CSI case, we use $\boldsymbol{\Sigma}_k = \sigma_e^2 \boldsymbol{I}$ and specify the error variance σ_e^2.

Figures 10 and 11 show the SINR performance for the FC system with robust precoder design according to the sum-MSE criterion. The results are shown as a function of the channel uncertainty and parametrized with DC bias I_{DC}. Setup II from Figure 5 with $x = 1.25$ and $y = 1.25$ is used to calculate the channel estimate $\hat{\boldsymbol{h}}_k$ and 5000 possible channel realizations $\boldsymbol{h}_k$ either according to the uncertainty bound ϵ_k or the normalized

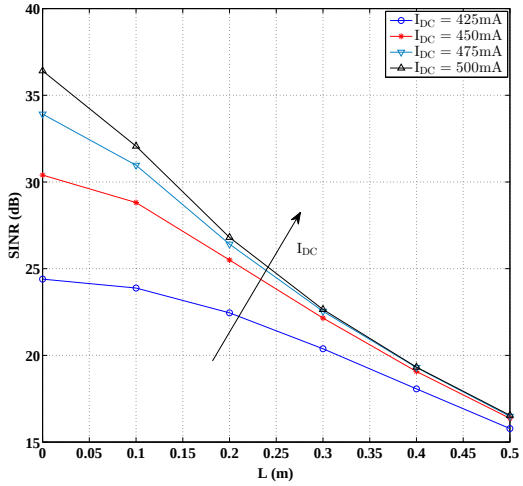

Figure 10: Robust sum-MSE minimization with outdated CSI. Setup II with $x = 1.25$ and $y = 1.25$.

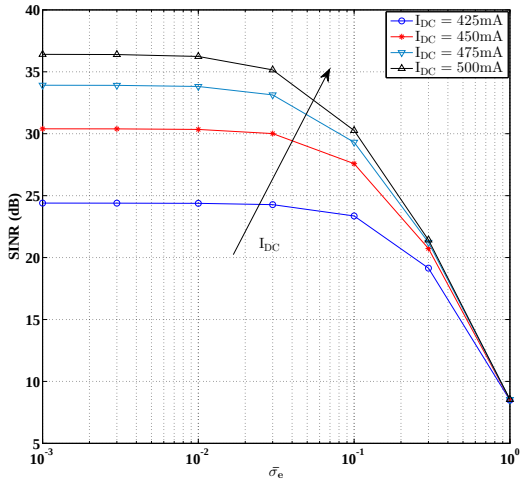

Figure 11: Robust sum-MSE minimization with noisy CSI. Setup II with $x = 1.25$ and $y = 1.25$.

error standard deviation $\bar{\sigma}_e = \sigma_e/(\|\text{vec}(\hat{\boldsymbol{H}})\|_1/(N_t N_r))$. The minimum achieved SINR among channel realizations is plotted for the case of outdated CSI, while the average SINR over channel realizations is plotted for the case of noisy CSI. From the figures, we can see that system performance improves as the DC bias I_{DC} increases, until the CSI uncertainty at the transmitter limits the SINR. Furthermore, the decline of SINR with uncertainty is less pronounced for the average performance measure considered in Figure 11. The worst-case optimization for the case of outdated CSI provides performance guarantees, which however diminish with increasing uncertainty, as shown in Figure 10.

D. Minimal Illumination Level Problem

We again consider the Setup II from Figure 5 with $x = 1.25$ and $y = 1.25$, and FC. Figure 12 shows the minimum illumination level, i.e., DC bias I_{DC}, that is required to meet the VLC MSE levels q_k of each user terminal. The

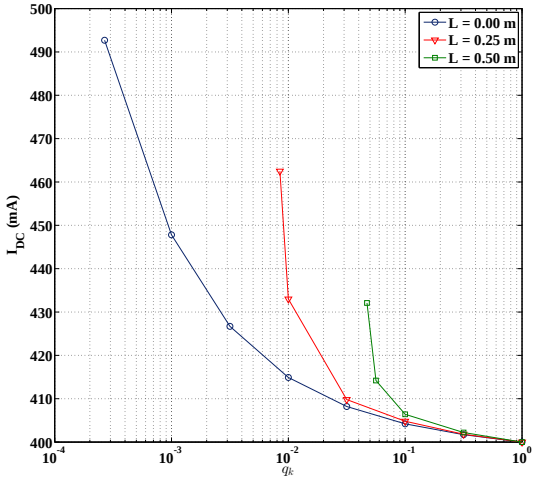

Figure 12: Robust illuminance minimization with perfect ($L = 0$) and outdated ($L > 0$) CSI. Setup II with $x = 1.25$ and $y = 1.25$.

different curves are for perfect CSI ($L = 0$) and outdated CSI ($L > 0$), and they quantify to what extent VLC is possible when lights are dimmed. The perfect CSI case shows the best possible trade-off between illumination level and achievable performance. When CSI uncertainty comes into play, it increases the required illumination level and eventually limits the achievable performance. That is, the larger the uncertainty region (quantified by L), the earlier the problem becomes infeasible, i.e., MSE constraints cannot be met regardless of illumination level.

E. Comparison between Robust and Non-Robust Design

Finally, we illustrate the benefits of the robust design in the case of CSI uncertainty. To this end, Figure 13 compares the SINR performances of the robust and non-robust precoder designs when CSI is outdated. Similar to Figure 9, SINR performance for one quadrant of the room is plotted as a function of the assumed user location, according to which $\hat{\boldsymbol{h}}_k$ is obtained. The actual user location is sampled in a circle with radius L, from which the channel gain $\boldsymbol{h}_k$ follows. Figure 13 shows, for each assumed location, the minimum SINR over the uncertainty region. The DC current I_{DC} is fixed as $I_{DC} = (I_L + I_U)/2$.

We observe that especially for locations close to the boundaries of two cells the robust design significantly outperforms the non-robust approach. This is due to the possibly large mismatch between assumed and actual channel gains, which also affects the expected amount of interference, and which is not taken into account in the non-robust design approach. For example, for the case of L=0.25, the average SINR value on the boundaries of two cells is improved from -25.99 dB to -0.69 dB via the robust design. On the other hand, closer inspection of the results shows that for locations further from the boundaries between cells, the precoder from the non-robust design achieves a somewhat better SINR than the robust precoder. For example, at the location $(x, y) = (0.375, 1.000)$,

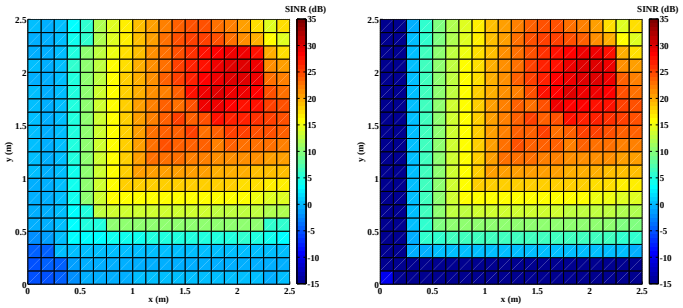

(a) Robust Design (L=0.25m) (b) Non-Robust Design (L=0.25m)

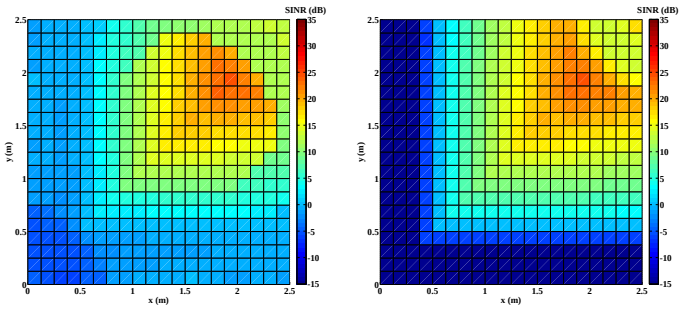

(c) Robust Design (L=0.5m) (d) Non-Robust Design (L=0.5m)

Figure 13: Comparison between robust and non-robust design for sum-MSE minimization problem with outdated CSI.

the worst-case SINR for the robust design is 4.4 dB, while it is 6.2 dB for the non-robust design. The reason for this is the conservativism of the robust design, which considers the worst case for all hypothetical gains from the bounded region $\mathcal{R}_k = \left\{ \boldsymbol{h}_k \;\middle|\; \begin{smallmatrix} \boldsymbol{h}_k = \hat{\boldsymbol{h}}_k + \boldsymbol{\delta}_k \\ \|\boldsymbol{\delta}_k\|_2 \leq \epsilon_k \end{smallmatrix} \right\}$, even though only a subset of these channel gains do actually occur inside the location uncertainty region. Nevertheless, the results in Figure 13 demonstrate the advantage of the robust optimization for VLC broadcasting in the case of imperfect CSI, in that the SINR is more consistently high over the entire attocell area and when different users are close to each other.

VI. Conclusion

In this paper, we have studied transmission to multiple user terminals using VLC attocells. Considering the inter-cell interference as a result of the broadcast nature of VLC, we have proposed the coordination of transmission in different attocells. These coordinated VLC attocells form CoMP-attocells, similar to CoMP-cells in RF cellular networks. We have derived new linear precoding schemes that reduce intra-CoMP-attocell interference with the objective of optimizing system performance given an illumination level and retaining a required performance at minimal illumination level, respectively. Our numerical results for a typical VLC scenario have clearly demonstrated the improvements of receiver-side SINR due to the proposed coordination. As a second important contribution, we have extended the precoding methods to include channel uncertainty, which would occur, for example, in the case of moving terminals. Simulation results have shown that these robust precoding schemes mitigate performance drops that stale channel information causes.

Acknowledgment

The authors would like to thank Mr. Warren Pawlikowski for his VLC noise measurements that helped choosing realistic parameters in this work.

References

[1] H. Ma, L. Lampe, and S. Hranilovic, "Robust MMSE linear precoding for visible light communication broadcasting systems," in *Workshop on Optical Wireless Communications, IEEE Global Communications Conference (Globecom)*, Atlanta, GA, USA, Dec. 2013.

[2] Cisco, "Cisco Service Provider Wi-Fi: A Platform for Business Innovation and Revenue Generation," http://www.cisco.com/en/US/solutions/collateral/ns341/ns524/ns673/solution_overview_c22-642482.html/, 2012, [Online; accessed 27-Dec-2013].

[3] S. Rajagopal, R. Roberts, and S. Lim, "IEEE 802.15.7 visible light communication: modulation schemes and dimming support," *IEEE Commun. Mag.*, vol. 50, no. 3, pp. 72–82, 2012.

[4] S. Hranilovic, L. Lampe, and S. Hosur, "Visible light communications: the road to standardization and commercialization (Part 1)," *IEEE Commun. Mag.*, vol. 51, no. 12, pp. 24–25, Dec. 2013.

[5] H. Haas, "High-speed wireless networking using visible light," *SPIE Newsroom*, Apr. 2013.

[6] H. C. Ferreira, L. Lampe, J. Newbury, and T. G. Swart, Eds., *Power Line Communications: Theory and Applications for Narrowband and Broadband Communications over Power Lines*. John Wiley & Sons Ltd, 2010.

[7] T. Komine and M. Nakagawa, "Integrated system of white LED visible-light communication and power-line communication," *IEEE Trans. Consumer Electron.*, vol. 49, no. 1, pp. 71–79, 2003.

[8] P. Amirshahi and M. Kavehrad, "Broadband access over medium and low voltage power-lines and use of white light emitting diodes for indoor communications," in *IEEE Consumer Communications & Networking Conference*, Las Vegas, Nevada, USA, 2006.

[9] A. Tonello, P. Siohan, A. Zeddam, and X. Mongaboure, "Challenges for 1 Gbps power line communications in home networks," in *IEEE International Symposium on Personal, Indoor and Mobile Radio Communications (PIMRC)*, Sep. 2008, pp. 1–6.

[10] H. Ma, L. Lampe, and S. Hranilovic, "Integration of indoor visible light and power line communication systems," in *IEEE International Symposium on Power Line Communications and Its Applications (ISPLC)*, 2013, pp. 291–296.

[11] R. Irmer, H. Droste, P. Marsch, M. Grieger, G. Fettweis, S. Brueck, H. P. Mayer, L. Thiele, and V. Jungnickel, "Coordinated multipoint: Concepts, performance, and field trial results," *IEEE Commun. Mag.*, vol. 49, no. 2, pp. 102–111, Feb. 2011.

[12] L. Zeng, D. O'Brien, H. Minh, G. Faulkner, K. Lee, D. Jung, Y. Oh, and E. Won, "High data rate multiple input multiple output (MIMO) optical wireless communications using white LED lighting," *IEEE J. Select. Areas Commun.*, vol. 27, no. 9, pp. 1654–1662, 2009.

[13] T. Fath and H. Haas, "Performance comparison of MIMO techniques for optical wireless communications in indoor environments," *IEEE Trans. Commun.*, vol. 61, no. 2, pp. 733–742, 2013.

[14] S. Serbetli and A. Yener, "Transceiver optimization for multiuser MIMO systems," *IEEE Trans. Signal Processing*, vol. 52, no. 1, pp. 214–226, 2004.

[15] V. Stankovic and M. Haardt, "Generalized design of multi-user MIMO precoding matrices," *IEEE Trans. Wireless Commun.*, vol. 7, no. 3, pp. 953–961, 2008.

[16] H. Huh, H. C. Papadopoulos, and G. Caire, "Multiuser MISO transmitter optimization for intercell interference mitigation," *IEEE Trans. Signal Processing*, vol. 58, no. 8, pp. 4272–4285, 2010.

[17] Z. Yu, R. J. Baxley, and G. T. Zhou, "Multi-user MISO broadcasting for indoor visible light communication," in *IEEE International Conference on Acoustics, Speech and Signal Processing (ICASSP)*, May 2013.

[18] J. Grubor, S. C. J. Lee, K.-D. Langer, T. Koonen, and J. W. Walewski, "Wireless high-speed data transmission with phosphorescent white-light leds," *ECOC 2007*, 2007.

[19] F. R. Gfeller and U. Bapst, "Wireless in-house data communication via diffuse infrared radiation," *Proceedings of the IEEE*, vol. 67, no. 11, pp. 1474–1486, 1979.

[20] T. Komine and M. Nakagawa, "Fundamental analysis for visible-light communication system using LED lights," *IEEE Trans. Consumer Electron.*, vol. 50, no. 1, pp. 100–107, 2004.

[21] S. D. Personick, "Receiver design for digital fiber optic communication systems, part I and II," *Bell system technical journal*, vol. 52, pp. 843–886, 1973.
[22] "IEEE standard for local and metropolitan area networks–part 15.7: Short-range wireless optical communication using visible light," *IEEE Std 802.15.7-2011*, pp. 1 –309, June 2011.
[23] H. Elgala, R. Mesleh, and H. Haas, "An LED model for intensity-modulated optical communication systems," *IEEE Photon. Technol. Lett.*, vol. 22, no. 11, pp. 835–837, 2010.
[24] C. W. Tan, M. Chiang, and R. Srikant, "Maximizing sum rate and minimizing MSE on multiuser downlink: optimality, fast algorithms and equivalence via max-min SINR," *IEEE Trans. Signal Processing*, vol. 59, no. 12, pp. 6127–6143, 2011.
[25] M. Joham, K. Kusume, M. H. Gzara, W. Utschick, and J. Nossek, "Transmit Wiener filter for the downlink of TDDDS-CDMA systems," in *IEEE Seventh International Symposium on Spread Spectrum Techniques and Applications*, vol. 1, 2002, pp. 9–13.
[26] J. Lofberg, "YALMIP: A toolbox for modeling and optimization in MATLAB," in *IEEE International Symposium on Computer Aided Control Systems Design*, 2004, pp. 284–289.
[27] M. Grant, S. Boyd, and Y. Ye, "CVX: Matlab software for disciplined convex programming," 2008.
[28] M. Shenouda and T. N. Davidson, "On the design of linear transceivers for multiuser systems with channel uncertainty," *IEEE J. Select. Areas Commun.*, vol. 26, no. 6, pp. 1015–1024, 2008.
[29] N. Vucic, H. Boche, and S. Shi, "Robust MSE-constrained downlink precoding in multiuser MIMO systems with channel uncertainty," in *45th Annual Allerton Conference on Communication, Control, and Computing, Monticello, IL, USA*, 2007.
[30] D. Tsonev, S. Videv, and H. Haas, "Light fidelity (Li-Fi): towards all-optical networking," in *SPIE 9007, Broadband Access Communication Technologies VIII*, Dec. 2013, pp. 900 702–900 702.
[31] W. Zhang and M. Kavehrad, "Comparison of VLC-based indoor positioning techniques," *Proc. SPIE*, vol. 8645, pp. 86 450M–86 450M–6, 2013.
[32] J. Armstrong, Y. Sekercioglu, and A. Neild, "Visible light positioning: a roadmap for international standardization," *IEEE Commun. Mag.*, vol. 51, no. 12, pp. 68–73, Dec. 2013.
[33] Y. C. Eldar, A. Ben-Tal, and A. Nemirovski, "Robust mean-squared error estimation in the presence of model uncertainties," *IEEE Trans. Signal Processing*, vol. 53, no. 1, pp. 168–181, 2005.
[34] Luxeon, http://www.luxeonstar.com/white-3985k-20mm-star-coolbase-led-190lm, [Online; accessed 27-June-2014].
[35] DIN, EN, "12464-1 (2011)," *Light and lighting. Lighting of work places. Part 1*.
[36] J. Grubor, S. Randel, K.-D. Langer, and J. W. Walewski, "Broadband information broadcasting using LED-based interior lighting," *J. Lightwave Technol.*, vol. 26, no. 24, pp. 3883–3892, 2008.
[37] E. D. Andersen, "Solving conic optimization problems with MOSEK," 2013.

Hao Ma (S'11) was born in Shandong, China. He received the B.S. degree in Information Engineering in 2010 from Xi'an Jiaotong University, Xi'an, China and M.S. degree in Electrical Engineering in 2012 from King Abdullah University of Science and Technology (KAUST), Thuwal, KSA. He is currently working toward his Ph.D. degree at the Department of Electrical and Computer Engineering, University of British Columbia (UBC), Vancouver, CA.

Lutz Lampe (M'02, SM'08) received the Dipl.-Ing. and Dr.-Ing. degrees in electrical engineering from the University of Erlangen, Erlangen, Germany, in 1998 and 2002, respectively. Since 2003, he has been with the Department of Electrical and Computer Engineering, University of British Columbia, Vancouver, BC, Canada, where he is a Full Professor. His research interests are broadly in theory and application of wireless, optical wireless and power line communications. Dr. Lampe was the General (Co-)Chair for 2005 ISPLC and 2009 IEEE ICUWB and General Co-Chair for the 2013 IEEE SmartGridComm. He is currently an Associate Editor of the IEEE WIRELESS COMMUNICATIONS LETTERS and the IEEE COMMUNICATIONS SURVEYS AND TUTORIALS and has served as an Associate Editor and a Guest Editor of several IEEE TRANSACTIONS and journals. He was a (co-)recipient of a number of Best Paper Awards, including awards at the 2006 IEEE International Conference on Ultra-Wideband (ICUWB), 2010 IEEE International Communications Conference (ICC), and 2011 IEEE International Conference on Power Line Communications (ISPLC).

Steve Hranilovic (S'94-M'03-SM'07) received the B.A.Sc. degree with honours in electrical engineering from the University of Waterloo, Canada in 1997 and M.A.Sc. and Ph.D. degrees in electrical engineering from the University of Toronto, Canada in 1999 and 2003 respectively.

He is an Associate Professor in the Department of Electrical and Computer Engineering, McMaster University, (Hamilton, ON, Canada), where he also serves as Associate Chair for undergraduate studies. During 2010-2011 he spent his research leave as Senior Member, Technical Staff in Advanced Technology for Research in Motion, Waterloo, Canada. His research interests are in the areas of free-space and wired optical communications, digital communication algorithms, and electronic and photonic implementation of coding and communication systems. He is the author of the book *Wireless Optical Communications Systems* (New York:Springer, 2004).

Dr. Hranilovic is a licensed Professional Engineer in the Province of Ontario and was awarded the Government of Ontario *Early Researcher Award*. He currently serves as an Associate Editor for the *IEEE Transactions on Communications* in the area of Optical Wireless Communications.